



Synthesis and structure–activity relationship studies of dihydronaphthyridinediones as a novel structural class of potent and selective PDE7 inhibitors

Rainer Gewalt*, Carla Rueger, Christian Grunwald, Ute Egerland, Norbert Hoefgen

biocrea GmbH, Meissner Strasse 191, 01445 Radebeul, Germany

ARTICLE INFO

Article history:

Received 19 August 2011

Revised 14 September 2011

Accepted 16 September 2011

Available online 21 September 2011

Keywords:

PDE7 inhibitor

Phosphodiesterase

Dihydronaphthyridinedione

Structure–activity relationship

Molecular docking

ABSTRACT

The synthesis and SAR studies of a series of structurally novel inhibitors of PDE7 are discussed. The best compounds from the series display low nanomolar inhibitory activity and are selective versus other PDE isoenzymes.

© 2011 Elsevier Ltd. All rights reserved.

Phosphodiesterase enzymes (PDEs) play an important role in various biological processes by hydrolyzing the key secondary messengers adenosine and guanosine 3',5'-cyclic monophosphates (cAMP and cGMP) into their corresponding 5'-monophosphate nucleotides, thereby decreasing concentrations of cAMP and cGMP, respectively.¹ At least eleven isoenzymes of mammalian cyclic nucleotide phosphodiesterase have been identified on the basis of primary structure, substrate specificity, or sensitivity to cofactors or inhibitory drugs.² Among them, PDE7 is a high affinity cAMP-specific PDE ($K_m = 0.2 \mu\text{M}$) with kinetic properties different from those of PDE4. The K_m of PDE7 is about 10-fold lower compared with PDE4. Interestingly, the inhibition of the activity or the expression of PDE7A was found to block the activation of T-cells as well as the proliferation and function of preactivated T-cells and cytotoxic T-lymphocytes.³ Recently, topical application of a PDE7A inhibitor in a mouse chronic inflammation model decreased the number of Ki67-positive keratinocytes, suggesting PDE7A to be a valuable therapeutic target of skin diseases, for example, psoriasis.⁴

As PDE7 inhibitors might also be useful in the treatment of CNS disorders,⁵ current medicinal chemistry effort are directed towards the identification of compounds active at very low concentrations.⁶ In order to avoid potential secondary effects such as emesis or cardiotoxicity, PDE isoenzyme selectivity is of great importance. In this context, high throughput screening of the compound

collection resulted in the identification of **1** as a weak dual PDE4/PDE7 inhibitor with IC_{50} values of 0.38 and 0.82 μM , respectively (Fig. 1).

This communication describes our preliminary efforts towards optimizing the enzymatic inhibitory activity and the selectivity profile of these compounds versus PDE4, which is also a cAMP-specific PDE.

During the initial phase of our work to evaluate the structure–activity relationship (SAR) of this new type of PDE7 inhibitors we investigated the role of substituents on the pyrido ring of the core structure. Surprisingly, we detected that the incorporation of a hydrogen bond acceptor function yielded very different effects on the target affinity of these derivatives. While the introduction of

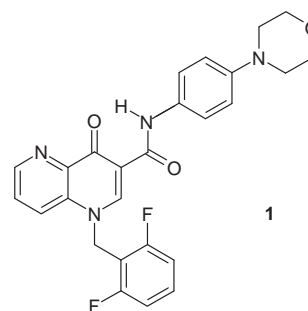


Figure 1. Structure of hit 1.

* Corresponding author. Tel.: +49 351 4043 1204.

E-mail address: rainer.gewald@biocrea.com (R. Gewalt).

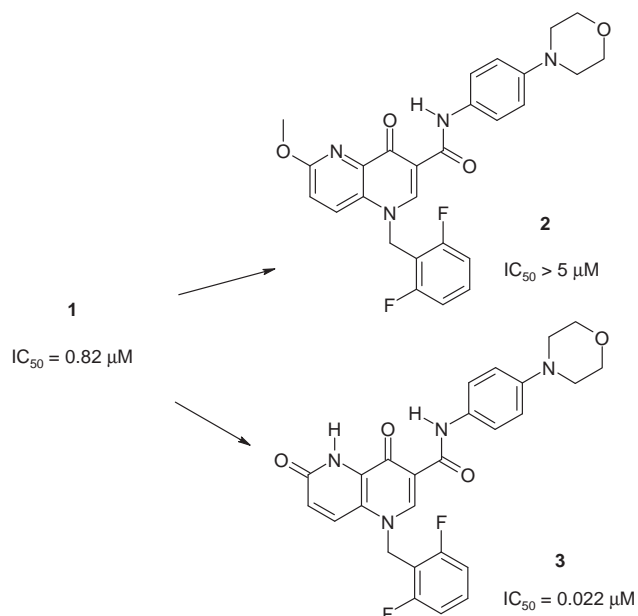


Figure 2. Structures of modified hit compounds **2** and **3**.

a methoxy group in 6-position created an inactive compound **2**, a carbonyl function at the same position as in compound **3** shifted the IC_{50} value to about 40-fold higher affinity (Fig. 2).

Since compounds **1**, **2**, and **3** display a wide range of potency but differ only regarding the substitution in the 6-position of the naphthyridine ring it is concluded that interaction of this part with the PDE7 catalytic domain is crucial for the target affinity. Molecular docking into the published co-crystal structure⁷ of PDE7 and 3-isobutyl-1-methylxanthine (IBMX) (PDB ID 1ZKL rev. 3.101) was used

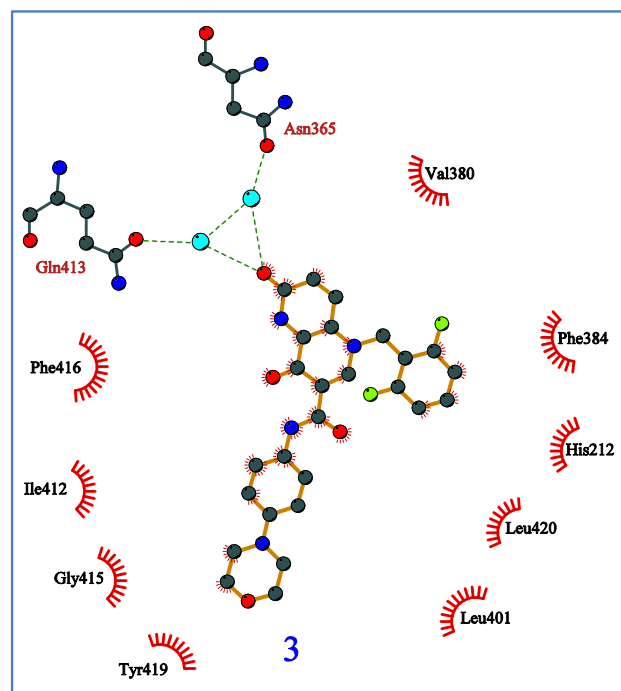
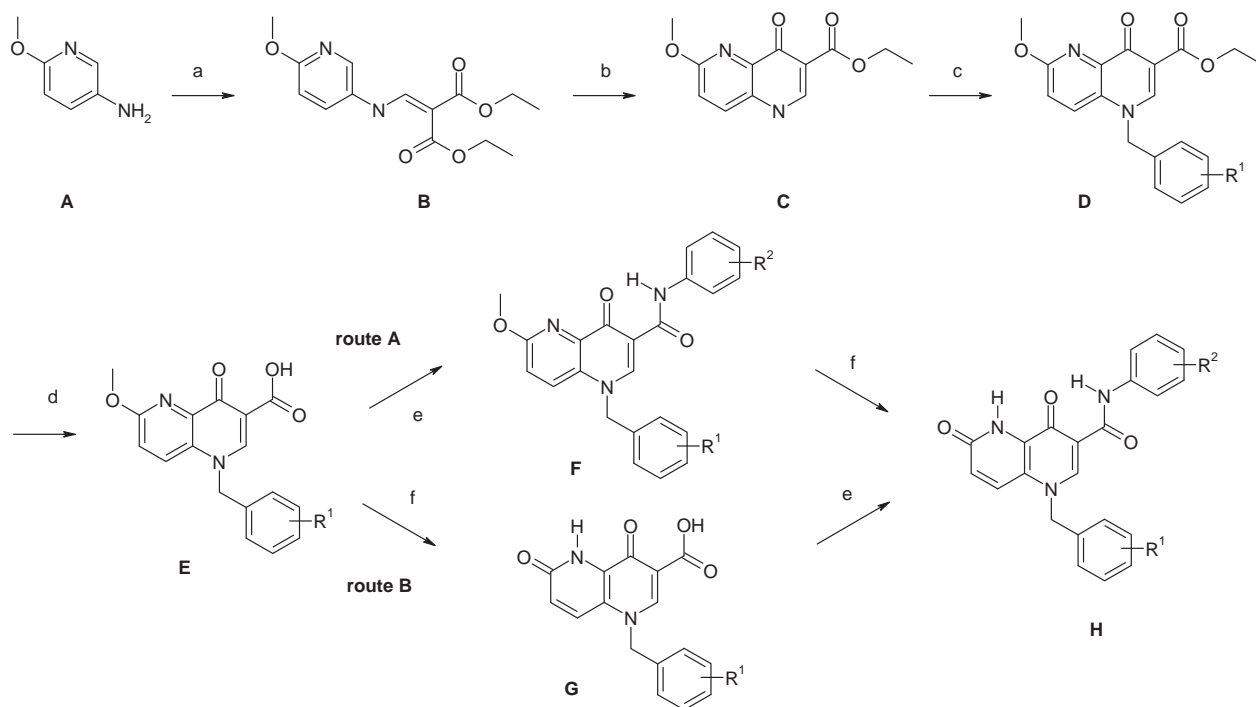


Figure 3. Schematic representation of GOLD docking result generated by LigPlot+.¹³ Water mediated hydrogen bonds are indicated by green dotted lines. Residues making nonbonded contacts with compound **3** are shown as spoked arcs.

to derive a reasonable hypothesis on the binding mode of these compounds. Prior to docking, conformation and tautomeric forms of compounds under study were analyzed applying semiempirical AM1 calculations.⁸ Results indicate (i) anti conformation of the two carboxy oxygens of our compounds and (ii) keto tautomerization



Scheme 1. Reagents and conditions: (a) $\text{EtOCH}(\text{COOEt})_2$, DMF, 120 °C, 92% yield; (b) $(\text{C}_6\text{H}_5)_2\text{O}$, reflux, 56% yield; (c) R^1 -substituted benzyl bromide, K_2CO_3 , DMF, 120 °C, 52–75% yield; (d) KOH, H_2O , EtOH, rt, 84–96% yield; (e) R^2 -substituted aniline, $\text{ClCOCH}_2\text{CH}(\text{CH}_3)_2$, Et_3N , CH_2Cl_2 , 0 °C to rt, 56–80% yield; (f) 48% aqueous HBr, AcOH, reflux, 72–95% yield.

of naphthyridine-diones. Both results are supported by NMR data which also indicate an internal hydrogen bond between the amide nitrogen and neighboring naphthyridine carboxy oxygen. These findings were used to constrain docking calculations employing the program GOLD.⁹

Figure 3 schematically depicts the interaction of compound **3** and the PDE 7 binding site derived from GOLD docking. A direct hydrogen bond to conserved Gln413 known from natural PDE substrates^{10,11} and most PDE inhibitors does not exist. Such interaction is prevented sterically and would be found only if the morpholine-phenyl-amide group was freely rotatable. Instead, docking calculations indicate two water-mediated hydrogen bond interactions of carboxy oxygen at 6-position and Gln413 and Asn365. The NH at the 5-position is not involved in such interactions according to the docking outcome. In addition to hydrogen bonds, the naphthyridine ring is held between Phe416, Val 380, and Phe384 known as the 'hydrophobic clamp'.¹² Compared with these results, no direct or mediated hydrogen bonding interactions of compounds **1** and **2**, respectively, with Gln413 were found, leading to a drop of affinity. Whereas **1** still fits into the hydrophobic clamp, steric interactions of the MeO group of **2** lead to a slight shift out of this region causing loss of affinity. Other interactions should not discriminate between compounds **1**, **2**, and **3**: There are a number of hydrophobic contacts with the morpholino-phenyl side chain. The morpholine ring sticks out of the binding site and thus will interact with surrounding polar solvent in a favorable way. Following our hypothesis that the carbonyl group in compound **3** is crucial for high target affinity and thus we focused our optimization strategy on the SAR of this type of inhibitor.

The 1,5-dihydro-[1,5]naphthyridine-2,8-dione derivatives were prepared as described in Scheme 1.

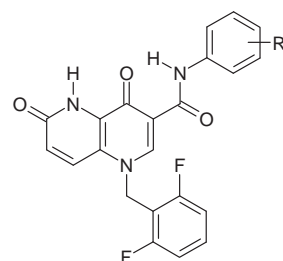
The synthesis of intermediates **E** followed established procedures for [1,5]naphthyridine ring synthesis.¹⁴ 5-Amino-2-methoxy-pyridine **A** was condensed with diethyl ethoxymethylenemalonate to afford the enamine **B**. Thermal cyclization of this enamine in refluxing diphenyl ether provided 1,4-dihydro[1,5]naphthyridine-3-carboxylic acid ethyl ester **C**, which was alkylated in the presence of potassium carbonate with substituted benzyl bromides to yield intermediates **D**. The corresponding carboxylic acids **E** were obtained by alkaline saponification. Depending on the stability of the functional groups R² either the amide formation was carried out at first followed by cleavage of the methoxy group (route A) or vice versa (route B). The coupling of the carboxylic acids **E** and **G** with substituted anilines was mediated by isobutyl chloroformate according to the mixed anhydride method of peptide synthesis.¹⁵ Formation of the second cyclic carbonyl function in intermediates **G** and target compounds **H** was brought about by using standard conditions for the cleavage of arylalkyl ethers with hydrogen bromide in acetic acid.¹⁶

The compounds described in this paper were assessed against both PDE7A and PDE7B subtypes. As no selectivity was observed, only the PDE7A inhibitory activities will be presented herein.

As a first approach, we decided to keep the substitution pattern at the benzyl group unchanged and focus on the amide part of the molecule. Using a parallel synthesis approach, a large number of different R² substituents were introduced at the phenyl ring and evaluated. Table 1 lists the structures and inhibitory activity of selected analogs from this series.

Replacement of the morpholine structure at the 4-position by a number of other amino groups (**4–9**) was tolerated, but with an apparent loss of selectivity in line with the decreasing size of the substituent. As inhibitory activity was found to be only slightly lower for nonsubstituted **10**, it became clear, that the modification of physicochemical properties by introducing a variety of other functional groups should be feasible.

Table 1
In vitro data for compounds **1–32**



Compd ^a	R ²	PDE7A1 ^b (IC ₅₀ , μM)	PDE4A4 ^b (IC ₅₀ , μM)
1 ¹⁷		0.823	0.379
2 ¹⁸		>5.00	>5.00
3	4-N-morpholinyl	0.022	0.506
4	4-N-piperidinyl	0.124	>1.00
5	4-NEt ₂	0.046	0.442
6	4-NMe ₂	0.066	0.471
7	4-NHMe	0.082	0.994
8	4-NH ₂	0.104	0.477
9	4-NHCOMe	0.024	0.362
10	H	0.094	1.33
11	4-CN	0.096	>1.00
12	3-CN	1.07	>1.00
13	4-F	0.179	>1.00
14	2,6-Di-F	>1.00	0.219
15	4-CF ₃	0.300	>1.00
16	4-COOH	0.200	1.52
17 ¹⁹	4-CH ₂ COOH	0.176	>1.00
18	4-COMe	0.029	>1.00
19	4-CONH ₂	0.049	0.201
20	4-CONHMe	0.029	0.560
21	4-CONHCH ₂ -4-Pyridyl	0.020	0.430
22	4-CO-N-morpholinyl	0.188	1.06
23	4-SO ₂ CH ₃	0.027	>1.00
24	4-SO ₂ NH ₂	0.034	0.458
25	4-SO ₂ NH-thiazol-2-yl	0.025	0.481
26	4-SMe	0.086	>1.00
27 ²⁰	4-OH	0.105	>1.00
28	4-OMe	0.151	>1.00
29	4-OCHF ₂	0.071	0.568
30	4-OCF ₃	0.090	>1.00
31	3,5-di-OMe	0.212	>1.00
32	3,4,5-Tri-OMe	0.018	0.516

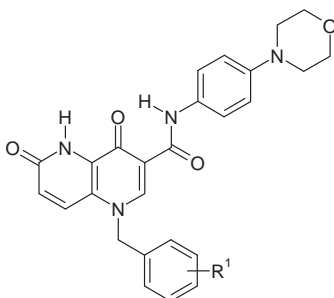
^a Compounds **1–26** prepared by route A; compounds **28–32** prepared by route B.

^b Measured against the human full length enzymes produced in baculovirus infected sf21 cells.²¹

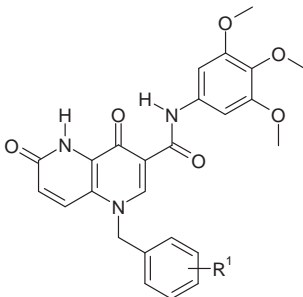
While small electron withdrawing functions such as cyano or fluorine (**11**, **13** and **15**) showed barely any influence on inhibitory activity, changing their position on the phenyl ring had a significant impact. When the point of attachment was moved from para to meta, an 11-fold loss in potency was observed (**12**). The fluorine disubstitution pattern in **14** even shifted the selectivity balance towards PDE4.

Further targeting the 4-position, the introduction of a carboxy group, connected either directly or by a methylene bridge, led to less active compounds (**16** and **17**). These results suggest an influence of pK_a as other carbonyl containing neutral groups (**18–21**) with the exception of tertiary amide **22** caused a flat SAR compared to **3**. However, the good selectivity exhibited by **18** turned into dual inhibition with the primary amide **19**. The sulfonyl derivatives **23–25** were found to maintain the level of activity in the same range as their carbonyl analogs.

None of the other mono and disubstituted neutral derivatives (**26–31**) provided any enhancement compared to reference compound **3**. Interestingly, the addition of a third methoxy group (**32**) reversed this trend.

Table 2
In vitro data for compounds **3** and **33–43**


Compd ^a	R ¹	PDE7A1 ^b (IC ₅₀ , μM)	PDE4A4 ^b (IC ₅₀ , μM)
3	2,6-di-F	0.022	0.506
33	H	0.712	>1.00
34	2-Me	0.266	>1.00
35	2-CF ₃	>1.00	>1.00
36	2-Cl	0.767	>1.00
37	2-Cl, 6-F	0.013	>1.00
38	2,6-di-Cl	0.165	>1.00
39	4-F	2.38	>5.00
40	4-OCF ₃	>1.00	>1.00
41	2,4-di-F	>1.00	>1.00
42	3,5-di-F	>1.00	>1.00
43	2,3,5,6-tetra-F	0.317	3.56

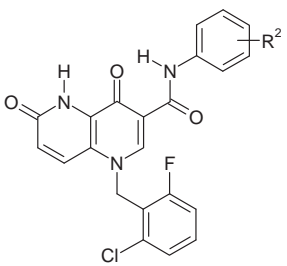
^a All compounds prepared by route A.^b Measured against the human full length enzyme produced in baculovirus infected sf21 cells.²¹**Table 3**
In vitro data for compounds **32** and **44–51**


Compd ^a	R ¹	PDE7A1 ^b (IC ₅₀ , μM)	PDE4A4 ^b (IC ₅₀ , μM)
32	2,6-di-F	0.018	0.516
44	2-Cl, 6-F	0.033	>1.00
45	H	0.686	>1.00
46	2-Cl	0.178	>1.00
47	2-F	0.206	>1.00
48	2-Br	>1.00	>1.00
49	2-Cl, 4-F	0.192	>1.00
50	2,6-di-Cl	0.088	0.979
51	4-F	0.868	>1.00

^a All compounds prepared by route B.^b Measured against the human full length enzyme produced in baculovirus infected sf21 cells.²¹

We next explored the SAR around the benzyl ring while retaining the morpholinophenyl substituent at the amide group (Table 2). Removal of the two fluorine atoms caused a large drop in potency (**33**). An *ortho* monosubstitution alone turned out not to be sufficient to regain high activity levels (**34–36**).

Consequently, we then evaluated the impact of the replacement of one or both fluoro by chloro substituents (**37** and **38**) leading to

Table 4
In vitro data for compounds **37** and **52–63**


Compd ^a	R ²	PDE7A1 ^b IC ₅₀ , μM	PDE4A4 ^b IC ₅₀ , μM
37	4-N-morpholinyl	0.013	>1.00 ^c
52	4-NEt ₂	0.060	>5.00 ^c
53	4-NMe ₂	0.039	0.402
54	4-NHCOMe	0.017	0.362
55	4-COMe	0.018	0.161
56	4-CONH ₂	0.010	0.090
57	3-CONH ₂	0.044	0.580
58	4-CONHMe	0.018	0.156
59	4-SO ₂ CH ₃	0.012	0.073
60	3-SO ₂ CH ₃	0.059	1.42
61	4-SO ₂ NH ₂	0.020	0.385
62	4-SO ₂ NH-thiazol-2-yl	0.032	0.274
63	3-Cl, 4-OMe	0.034	>1.00

^a Compounds **37** and **52–62** prepared by route A; compound **63** prepared by route B.^b Measured against the human full length enzyme produced in baculovirus infected sf21 cells.²¹^c Applies also to human recombinant PDE1B, 2A, 3A, 5A and 8A–11A, and to PDE6 from bovine retina.

the most potent PDE7 inhibitor **37** with a selectivity ratio greater than 77 versus PDE4A.

Substitution at the *para* position was shown to be detrimental to the enzymatic activity (**39–41**), while a different arrangement or an increase in the number of F groups (**42** and **43**) was also not beneficial.

As **32** did not much differ in terms of activity and stability from the reference compound **3** we decided to verify the optimal substitution pattern at the benzyl moiety with the preparation of a further small subseries (Table 3).

Except for **46**, a similar tendency to that presented in Table 2 was observed. The fivefold improvement in potency prompted us to investigate in more detail *ortho* halo substituted derivatives (**47–50**) but the preferred substituent arrangements still remained with those found in **32** and **44**.

Finally, the most promising structural features from the previous subseries were combined to complete the SAR studies (Table 4). Synergistic effects with regard to selectivity versus PDE4 could particularly be demonstrated with compound **52** (>83-fold).

In general, smaller groups than dimethylamino caused a significant drop in selectivity (**53–61**) with ratios varying from 6- to 24-fold. Shifting the functionality from *para* to *meta* position (**57** and **60**) resulted again in a loss of activity, although this time the impact was less pronounced. The trimethoxy substitution pattern (**44**) could be replaced while maintaining affinity by the introduction of a 3-chloro, 4-methoxy template (**63**).

With the exception of **52** and **62** all compounds were slightly more potent compared to their analogs presented in Table 1.

In summary, the dihydronaphthyridinedione derivatives represent a new class of PDE7 inhibitors. A significant improvement in activity and selectivity was achieved starting from the weak dual PDE4/PDE7 inhibitor hit compound **1** by using molecular modeling

and modification of R¹ and R² chemical groups. The best compounds tested **37** and **52** displayed low nanomolar inhibitory activity and also showed good selectivity versus all other PDE isoenzymes. Further optimization of these newly discovered leads will be supported by the findings from this study.

Acknowledgments

The project was supported by the European Fund for Regional Development (EFRE) and the Free State of Saxony (SAB 8093).

References and notes

- (a) Beavo, J. A. *Physiol. Rev.* **1995**, *75*, 725; (b) Conti, M. In *Principles of Molecular Regulation*; Conn, P. M., Means, A. R., Eds.; Humana, 2000; pp 261–275; (c) Soderling, S. H.; Beavo, J. A. *Curr. Opin. Cell Biol.* **2000**, *12*, 174.
- (a) Soderling, S. H.; Bayuga, S. J.; Beavo, J. A. *J. Biol. Chem.* **1998**, *273*, 15553; (b) Conti, M.; Jin, S. L. C. In *Progress in Nucleic Acid Research and Molecular Biology*; Moldave, K., Ed.; Academic Press: New York, 1999; Vol. 63, pp 1–38.
- (a) Liu, Y.; Goff, R. D.; Zhou, D.; Mattner, J.; Sullivan, B. A.; Khurana, A.; Cantu, C., III; Ravkov, E. V.; Ibegbu, C. C.; Altman, J. D.; Teyton, L.; Bendelac, A.; Savage, P. B. *J. Immunol. Methods* **2006**, *312*, 34; (b) Kadoshima-Yamaoka, K.; Murakawa, M.; Goto, M.; Tanaka, Y.; Inoue, H.; Murafuji, H.; Nagahira, A.; Hayashi, J.; Nagahira, K.; Miura, K.; Nakatsuka, T.; Chamoto, K.; Fukuda, Y.; Nishimura, T. *Immunity Lett.* **2009**, *122*, 193; (c) Kadoshima-Yamaoka, K.; Murakawa, M.; Goto, M.; Tanaka, Y.; Inoue, H.; Murafuji, H.; Nagahira, A.; Hayashi, J.; Nagahira, K.; Miura, K.; Nakatsuka, T.; Chamoto, K.; Fukuda, Y.; Nishimura, T. *Int. Immunopharmacol.* **2009**, *9*, 97.
- Goto, M.; Kadoshima-Yamaoka, K.; Murakawa, M.; Yoshioka, R.; Tanaka, Y.; Inoue, H.; Murafuji, H.; Kanki, S.; Hayashi, J.; Nagahira, K.; Ogata, A.; Nakatsuka, T.; Fukuda, Y. *Eur. J. Pharmacol.* **2010**, *633*, 93.
- (a) Perez-Torres, S.; Cortes, R.; Tolnay, M.; Probst, A.; Palacios, J. M.; Mengod, G. *Exp. Neurol.* **2003**, *182*, 322; (b) de Gortari, P.; Mengod, G. *Brain Res.* **2010**, *1310*, 37; (c) Bergmann, J. E.; Cutshall, N. S.; Demopoulos, G. A.; Florio, V. A.; Gaitanaris, G.; Gray, P.; Hohmann, J.; Onrust, R.; Zeng, H. PCT Int. Appl. WO 129036 A1, 2010.
- (a) Vergne, F.; Bernardelli, P.; Chevalier, E. *Annu. Rep. Med. Chem.* **2005**, *40*, 227; (b) Gil, C.; Campillo, N. E.; Perez, D. I.; Martinez, A. *Expert Opin. Ther. Patents* **2008**, *18*, 1127.
- Wang, H.; Liu, Y.; Chen, Y.; Robinson, H.; Ke, H. *J. Biol. Chem.* **2005**, *280*, 30949.
- Clark, T., Alex, A., Beck, B., Chandrasekhar, J., Gedeck, P., Horn, A., Hutter, M., Martin, B., Rauhut, G., Sauer, W., Schindler, T., and Steinke, T. *vAMP* (version 7.5a). 1999, The Oxford Molecular Group, The Medawar Centre, Oxford Science Park, Oxford OX4 4GA, UK.
- GOLD (version 5.0.1). 2011, CCDC Software Ltd, Cambridge.
- Conti, M. *Nat. Struct. Mol. Biol.* **2004**, *11*, 809.
- Ke, H.; Wang, H. *Curr. Top. Med. Chem.* **2007**, *7*, 391.
- Zhang, K. Y.; Card, G. L.; Suzuki, Y.; Artis, D. R.; Fong, D.; Gillette, S.; Hsieh, D.; Neiman, J.; West, B. L.; Zhang, C.; Milburn, M. V.; Kim, S. H.; Schlessinger, J.; Bollag, G. *Mol. Cell* **2004**, *15*, 279.
- Wallace, A. C.; Laskowski, R. A.; Thornton, J. M. *Prot. Eng.* **1995**, *8*, 127.
- Heindl, J.; Kelm, H.-W.; Dogs, E.; Seeger, A.; Herrmann, C. *Eur. J. Med. Chem. Chim. Ther.* **1977**, *12*, 549.
- Hoffmann, J. A.; Tilak, M. A. *Org. Prep. Proced. Int.* **1975**, *7*, 215.
- Burwell, R. L., Jr. *Chem. Rev.* **1954**, *54*, 615.
- Prepared by using 2-aminopyridine as starting material instead of **A**.
- Corresponds to precursor **F** in the preparation of **3**.
- Prepared from the corresponding ethyl ester intermediate **F**.
- Prepared from **28** (BBr₃, CH₂Cl₂, reflux).
- PDE assays: PDE4A1 and PDE7A1 enzymes were generated from full-length recombinant human clones, expressed in Sf21 cells. The enzymatic activity was determined using a plate based Scintillation Proximity Assay (SPA) at a substrate concentration of 20 nM and 500 nM [³H]-cAMP for PDE7A1 and PDE4A4, respectively. The incubation in 80 mM Tris/10 mM MgSO₄ (pH 7.4) was allowed to proceed for 30 min at 37 °C before addition of 25 μl of the SPA beads. Plates were counted in a Trilux plate reader. The background was determined without enzyme for PDE7A1 and in the presence of 10 μM Rolipram for PDE4A4, respectively. IC₅₀ values are means of at least four experiments.